Progress In Electromagnetics Research M, Vol. 28, 129–143, 2013

EFFECTS OF ANTENNA DESIGN PARAMETERS ON THE CHARACTERISTICS OF A TERAHERTZ COPLANAR STRIPLINE DIPOLE ANTENNA

Truong Khang Nguyen and Ikmo Park*

School of Electrical and Computer Engineering, Ajou University, 5 Woncheon-dong, Youngtong-gu, Suwon 443-749, Korea

Abstract—This paper presents the antenna design parameter dependency on the impedance and radiation characteristics of a terahertz coplanar stripline dipole antenna. The antenna response is numerically investigated by applying a semi-infinite substrate and by generating a constant voltage source to drive a signal on the antenna. In this way, we can analyze the antenna characteristics without the photoconductive material response and the substrate lens geometrical effects. Further, we explain the mechanism underlying the preferable uses of several millimeter length DC bias striplines in a typical THz coplanar stripline dipole antenna design. The antenna, consisting of a center dipole connected to long bias striplines, has a traveling wave characteristic supporting an attenuated current, rather than a resonant characteristic supporting a standing wave of current. The traveling wave behavior produces stable antenna input impedances and minimal changes in the antenna radiation patterns. We also found that the length of the center dipole has a prominent effect on the antenna gain response.

1. INTRODUCTION

After the pioneering works by Jayaraman and Lee [1, 2], Auston et al. [3, 4], and Grischkowsky et al. [5], the techniques for generating and detecting terahertz (THz) radiation using femtosecond laser pulses have been studied extensively. There are several methods for generating and detecting THz electromagnetic waves, such as photoconductive switching, optical rectification, photomixing, quantum cascade lasers, free electron lasers, and backward wave

Received 24 November 2012, Accepted 9 January 2013, Scheduled 17 January 2013
* Corresponding author: Ikmo Park (ipark@ajou.ac.kr).

oscillator [6–10]. Among them, the method involving the use of a photoconductive switch (antenna), which typically consists of a metallic antenna patterned on a high-mobility semiconductor substrate, is the simplest and the most widely used THz wave generation method for producing a continuous spectrum up to a few THz upon exposure to an ultrashort laser pulse [11].

The photoconductive antenna plays an important role in the radiation of the THz wave, and numerous theoretical and experimental studies have been conducted on it. Various antenna designs, such as bow-tie [12], logarithm spiral [13], strip line [14], strip line dipole [15, 16], and fractal-based antennas [17, 18], have received significant attention for better generation and detection of THz radiation [19]. One of the most popular designs is the one that involves the use of a stripline dipole antenna, in which a center dipole is connected to coplanar striplines and forms an H-shaped electrode structure. This type of a coplanar stripline dipole antenna is well known as Grishkowsky's antenna [20, 21] and is preferable because of its simple structure and most successful commercial applications [22]. Theoretically, the dipole antenna is a resonance structure and supports a standing wave of current. However, the current distribution can be altered to support a traveling wave with attenuation while traveling from the feed point to the terminations of the dipole arms [23, 24]. This is true for photoconductive antennas possessing very long DC bias striplines with open-circuited terminations in a high dielectric constant substrate, because there is little current to be reflected back owing to the radiation as the current travels along the long striplines.

In this study, we investigate the effects of the DC bias striplines and the center dipole on the coplanar stripline dipole antenna in terms of the input impedance and radiation characteristics. The antenna response is investigated by applying a semi-infinite gallium-arsenide (GaAs) substrate and by generating a constant voltage source to drive a signal on the antenna. The former approach is employed because the semi-infinite substrate has been proven to show similar antenna resonant characteristics as lens substrates [25]. Moreover, the lens substrate exhibits frequency dependence of the antenna radiation property [26, 27]. The later approach of using a constant voltage source allows the characterization of the antenna response itself while ignoring the response of the photoconductive material to the optical signal. It is necessary to establish these simplifying conditions in order to fully characterize the antenna properties. Furthermore, once the underlying mechanism has been elucidated, appropriate DC bias lines can be modeled for better operation in THz coplanar stripline antenna designs.

2. ANTENNA DESIGN

The geometry of the coplanar stripline dipole antenna is shown in Figure 1. The antenna was designed on a semi-infinite GaAs substrate, where this substrate was approximated with a semi-infinite Green's function layer. The center dipole is designed to resonate at around 1.0 THz. Therefore, the resonant length of the center dipole should be approximately

$$L = \frac{\lambda_{eff}}{2} = \frac{1}{2}\frac{\lambda_0}{\sqrt{\frac{\varepsilon_r+1}{2}}} \tag{1}$$

where λ_0 is the free-space wavelength and ε_r the relative dielectric constant of GaAs ($\varepsilon_r = 12.94$). The width and the length of the center dipole are w_d and L_d, respectively, whereas those of the bias striplines are w_b and L_b, respectively. The metallic layer, as defined in the simulation, had a thickness of 0.35 µm and a conductivity of 1.6×10^7 S/m. In the gap, g, of the two-arm dipole, a wire port with a constant voltage source of magnitude 1 V is introduced to drive a signal on the antenna. The initial parameters for study of the effect of the bias line are $L_d = 40$ µm, $w_d = 10$ µm, $g = 5$ µm, and $w_b = 5$ µm. The method of a moment simulator FEKO was used to numerically investigate the characteristics of the antenna.

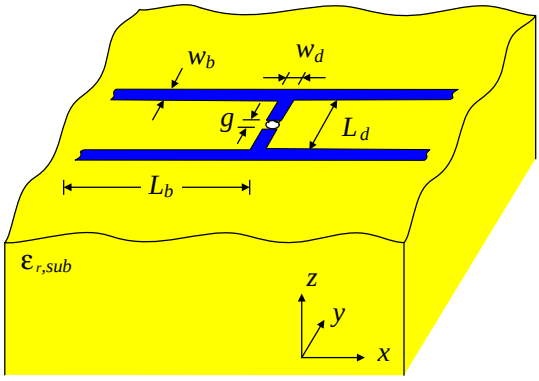

Figure 1. Photoconductive antenna structure.

3. ANTENNA CHARACTERISTICS

3.1. Bias Line Length Effect

GaAs substrates supporting terahertz chips usually are of 20×10 mm size such that sufficient space is ensured for the alignment of the silicon substrate lens on the back of the device. The standard lens diameter used in experiments is 10 mm, given that smaller sizes are not practical owing to the cut-off at low frequencies [28]. Consequently, the coplanar striplines for an external DC current bias have also been several millimeters long. Thus far, researchers have used such bias lines for as long as it is possible within the available chip area and have not fully understood about their impact. For our purposes, it is necessary to provide a thorough study on the bias line effect from the antenna perspective.

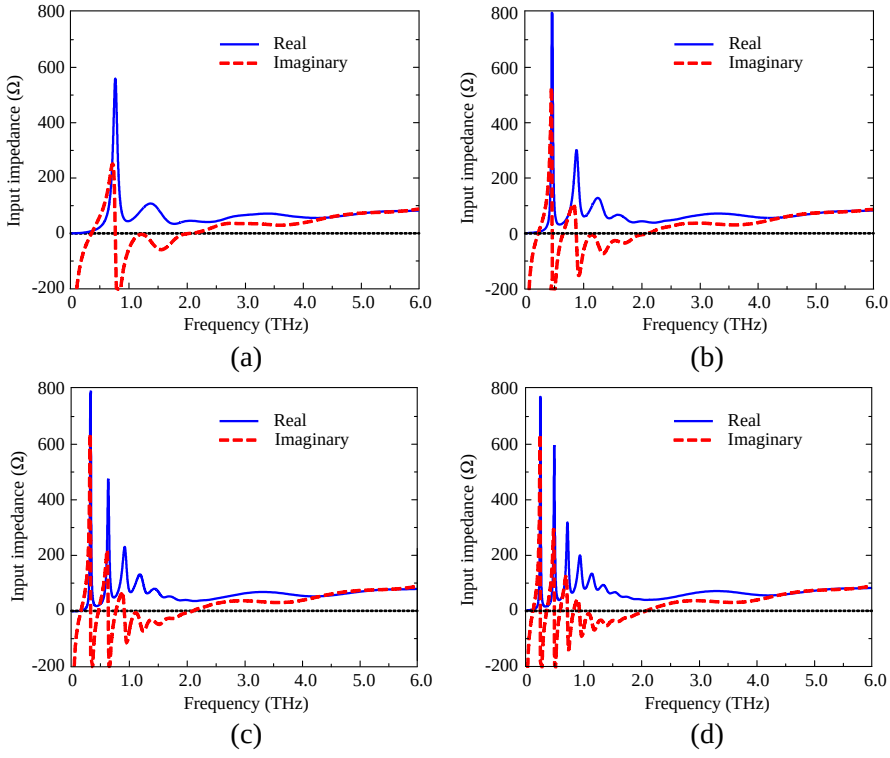

Figure 2. Input impedance characteristics of the antenna (L_d = 40 μm) with respect to the change in the bias line length L_b: (a) L_b = 50 μm, (b) L_b = 100 μm, (c) L_b = 150 μm, and (d) L_b = 200 μm.

We first studied the input impedance of the antenna when a bias line a few hundred micrometers in length, i.e., L_b = 50 µm, 100 µm, 150 µm and 200 µm, was used. Though these lengths are not practical for use in an actual device, our study has clearly shown the resonance behavior of the antenna using short bias lines. Figure 2 shows the input impedance characteristics of the antenna as the bias line length increases from 50 µm to 200 µm. As expected, the bias line affected the

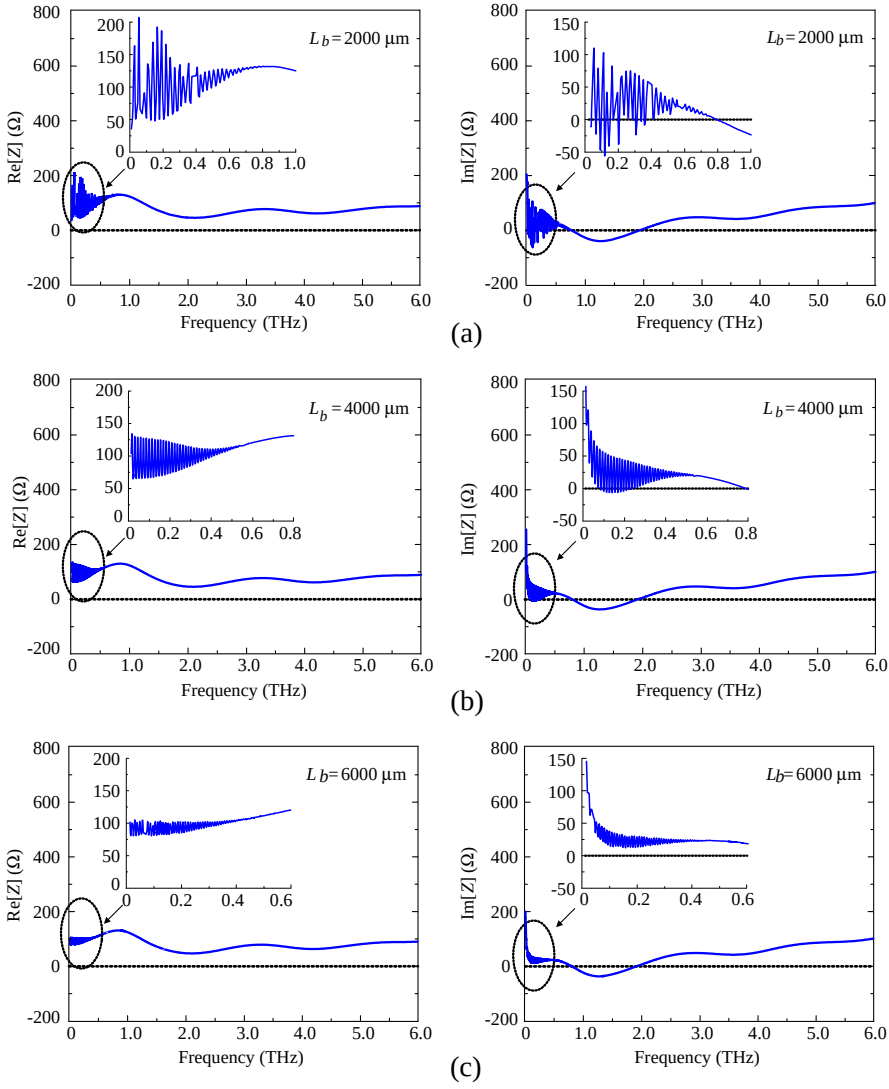

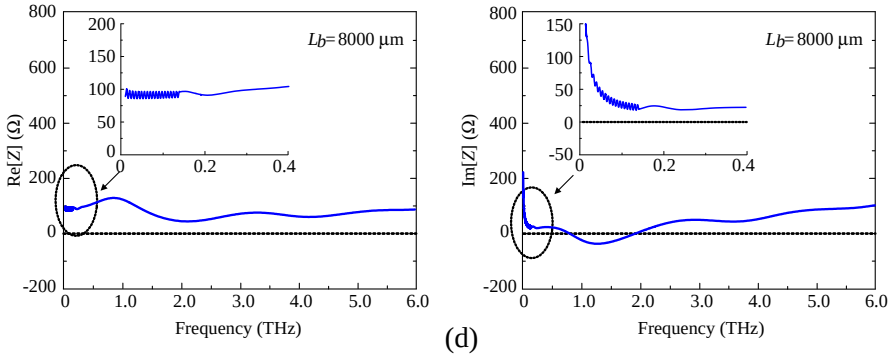

Figure 3. Input impedance characteristics of the antenna (L_d = 40 μm) with respect to the change in the bias line length L_b: (a) L_b = 2000 μm, (b) L_b = 4000 μm, (c) L_b = 6000 μm, and (d) L_b = 8000 μm. The insets show zoomed-in views at low frequencies.

resonant response of the antenna, and consequently, the fundamental resonance frequency decreased significantly. The imaginary part of the antenna impedance clearly showed the fundamental resonance frequency of the antenna, i.e., the point where the imaginary part of the impedance equals 0, was 0.3 THz, 0.2 THz, 0.13 THz, and 0.1 THz with bias line lengths of 50 μm, 100 μm, 150 μm, and 200 μm, respectively. In comparison with the original resonance frequency of the center dipole designed at 1.0 THz, we observed a considerable reduction in the resonance frequency. The periodic fluctuation of the antenna impedance in the low frequency region was clearer with respect to the increasing bias line length. This result is attributed to the multiple frequency mode operation. These frequency modes come close together and as a result cause fluctuation in the antenna input impedance at low frequencies. Therefore, the coplanar stripline dipole antenna with a short bias line scheme can be characterized as a standing wave antenna or a resonant antenna owing to the reflections at the bias line terminations. These observations confirm that the bias line in a typical THz coplanar stripline dipole antenna has certain effects on the input impedance and resonance frequency.

We further investigated the antenna characteristics when millimeter-long bias lines were used. Figure 3 shows the antenna input impedance when the bias line lengths were L_b = 2000 μm, 4000 μm, 6000 μm, and 8000 μm. The fluctuation of the input impedance at the low frequency region gradually reduced with an increase in the bias line length, while the antenna impedances in the high frequency region remained constant regardless of the bias line length. For the case of

$L_b = 2000\,\mu m$, the fluctuation amplitude of the resistance exceeded approximately $150\,\Omega$, and the frequency for the cut-off fluctuation was approximately 0.8 THz. When the antenna bias line length was $4000\,\mu m$ or $6000\,\mu m$, the fluctuation amplitude reduced significantly, e.g., to approximately $100\,\Omega$ for $L_b = 4000\,\mu m$ and to less than $50\,\Omega$ for $L_b = 6000\,\mu m$. In addition, the frequency for the cut-off fluctuation decreased with an increase in the bias line length. For instance, the frequency for a cut-off fluctuation of $L_b = 4000\,\mu m$ is approximately 0.6 THz and that for $L_b = 6000\,\mu m$ is approximately 0.4 THz. As a result, the longer bias line produced stable antenna impedance at low frequencies. Particularly, the bias line length of $L_b = 8000\,\mu m$ exhibited smooth impedance variations in both the resistance and the reactance response of the antenna. The imaginary part of the impedance oscillated slowly around $0\,\Omega$ with an amplitude of $\pm 50\,\Omega$ for the frequency range of 0–4 THz. The impedance of the antenna at low frequencies is immune to rippling for a sufficiently long bias line. This behavior can be explained on the basis of the traveling wave antenna theory in that the current attenuates as it travels along the bias line, leaving behind very little current to be reflected back at the bias line terminations. This is particularly true and obvious in the case of a high dielectric constant substrate material given that the effective wavelength traveling along the dipole arm is small in comparison with the free space wavelength.

To verify this traveling wave behavior of the antenna, the magnitude of the surface current was calculated along the bias line ($L_b = 8000\,\mu m$) and checked at different frequencies, as illustrated in Figure 4. At low frequencies of 0.1 THz and 0.4 THz, i.e., the very long

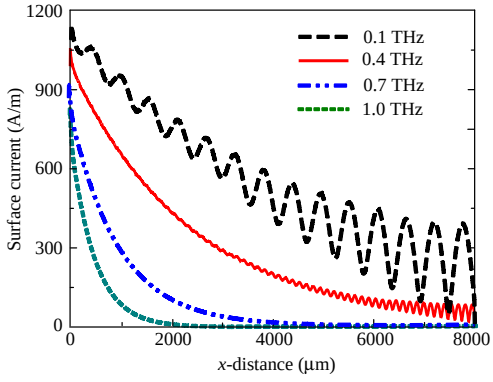

Figure 4. Current distribution along the bias lines ($L_b = 8000\,\mu m$) of the antenna ($L_d = 40\,\mu m$) calculated at different frequencies.

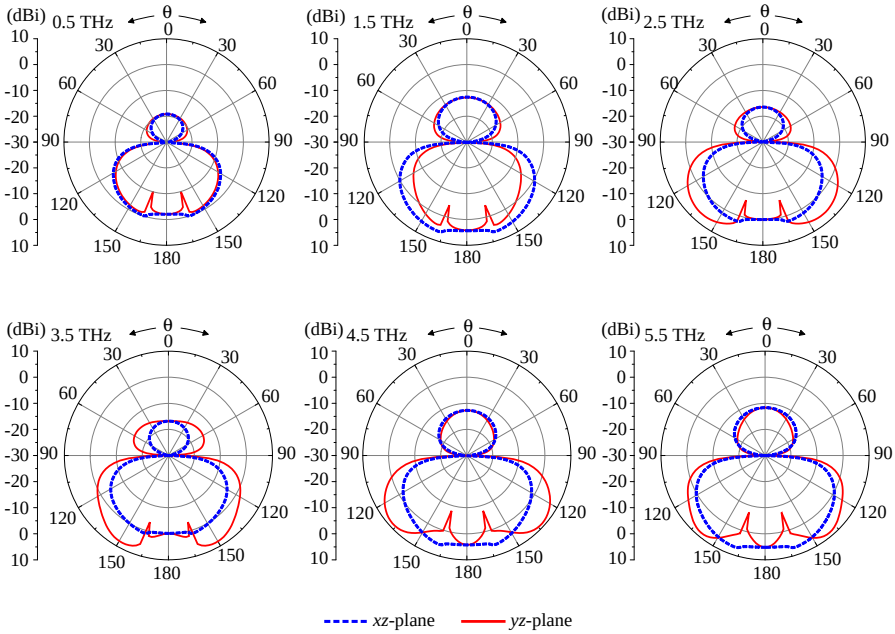

Figure 5. Radiation patterns at various frequencies of the antenna ($L_d = 40\,\mu\text{m}$) with a bias line length of $L_b = 8000\,\mu\text{m}$.

wavelengths, the current showed significant reflections at the bias line terminations, particularly for the case of the 0.1-THz frequency, and thus formed a standing wave. However, at higher frequencies of 0.7 THz and 1.0 THz, the current attenuated rapidly along the bias line, and as a result, reflection from the bias line terminations was completely eliminated. For instance, the current at 0.7 THz dropped to near zero level at approximately 4000 μm away from the feed point while that at 1.0 THz did so at a distance of only approximately 2000 μm. These observations indicate the necessity of using a sufficiently long bias line for operation at very low frequencies. On the other hand, a short bias line for a compact device is preferable for antennas operating at high frequencies.

Figure 5 shows the radiation patterns of the antenna at various frequencies, i.e., from 0.5 to 5.5 THz in 1 THz increments, for the case of $L_b = 8000\,\mu\text{m}$. The antennas exhibited radiation patterns with a maximum in the *xz*-plane and a minimum in the *yz*-plane at the critical angle $\theta_c = \pi - \sin^{-1}\left[(\varepsilon_r)^{-1/2}\right]$ on the dielectric side, which is approximately 164° for the GaAs substrate ($\varepsilon_r = 12.94$) [29]. The *xz*-plane patterns showed dipole-like radiation patterns and

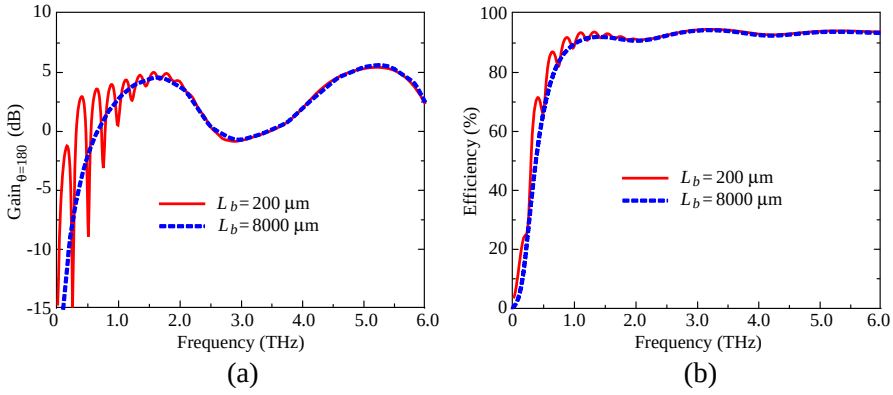

Figure 6. (a) Gain (checked at $\theta = 180°$) and (b) efficiency of the antenna ($L_d = 40\,\mu m$) with different bias line lengths.

maintained them over the entire frequency range of interest, but with a different maximum gain at $\theta = 180°$. However, the yz-plane patterns behaved differently with degraded radiation characteristics as the frequency increased. At high frequencies, the radiated power was not concentrated at the $\theta = 180°$ line, but it rather spread to neighbor lobes, e.g., $\pm 150°$ lobes for yz-plane pattern at 3.5 THz and $\pm 135°$ for the yz-plane pattern at 4.5 THz. This behavior is attributed to the higher order modes generated along the center dipole at high frequencies. In general, as the frequency varied, the radiation along the bias line direction, i.e., the xz-plane, exhibited minimal changes, corresponding to the radiation characteristic of a traveling wave antenna. However, the radiation along the dipole center direction, i.e., the yz-plane, varied substantially and showed an increased degree of degradation with an increase in the frequency.

Figure 6 shows the gain (at $\theta = 180°$) and the efficiency of the antenna for two representative bias line lengths, i.e., $L_b = 200\,\mu m$ and $L_b = 8000\,\mu m$. The antenna efficiency is defined as the ratio of the power radiated by the antenna to the power supplied to the antenna, and the gain is calculated assuming a perfect impedance matching condition. Generally, the gain of the antenna was low at the lower limit of the frequency range, i.e., 0–0.5 THz, because the effective antenna size became small relative to these long wavelengths. With a short bias line, the antenna gain exhibited resonant behavior with significant fluctuations in the low frequency range. The successive peaks and dips in the gain spectrum in this low frequency range are related to the resonant resistance and reactance

of the antenna. This phenomenon was diminished by extending the bias line, and it completely disappeared for the very long bias line lengths. As a result, antennas with sufficiently long bias lines achieved frequency-independent behavior with stable gain characteristics at low frequencies. In the high frequency range of 1–6 THz, a periodic variation of the antenna gain was observed. The gain spectrum had two peaks at 1.6 THz and 5.1 THz, with the approximate values of 4 dBi and 5 dBi, respectively. A minimum between the peaks was at the frequency of 3.0 THz with approximate value of −1.2 dBi. The average antenna gain is relatively low at approximately 1.2 dB, because the field strength produced by a traveling wave antenna is only one-third of that produced by a standing wave antenna, with the same length and feed excitation [30]. The multiple peak phenomena of the gain spectrum are explained using the radiation patterns shown in Figure 5. The maximum antenna gain was obtained when the radiated power focused at the $\theta = 180^\circ$ line, e.g., at 1.5 THz and 5.5 THz. The minimum of the gain spectrum resulted from the dispersion of the radiated power elsewhere rather than concentrating at the $\theta = 180^\circ$ line, e.g., at 3.5 THz. This effect is related to the resonance length of the antenna at the point where maximum radiation along the $\theta = 180^\circ$ direction occurs [31]. The efficiency of the antenna with two different bias line lengths showed similar trends, rapidly increasing from a few percent to more than 80% in the 0–1 THz frequency range and achieving saturation (with an average value of approximately 94%) in a wide frequency range from 1 THz to 6 THz. It is obvious that the efficiency at low frequencies was immune to the rippling caused by resonant behavior when a sufficiently long bias line was used. These investigations indicate the necessity of using long bias lines in the design of typical H-shaped coplanar stripline antennas if one is to achieve good radiation performance, particularly in the low operating frequency region of less than 1.0 THz.

3.2. Center Dipole Length Effect

The antenna characteristics with respect to the change in the center dipole length, L_d, were investigated, where the bias line length L_b was chosen as 8000 μm. As the length of the center dipole increased, i.e., from 20 μm to 40 μm to 80 μm to 160 μm, the variation in the input impedance of the antenna became more distinct at low frequencies (see Figure 7). The frequencies, where the imaginary part of the impedance equals to 0, were gradually decreased with an increase in the center dipole length. This behavior is similar to that observed for the short bias line study. This finding indicates that further increasing the center dipole length could lower the cut off frequency and thus produce

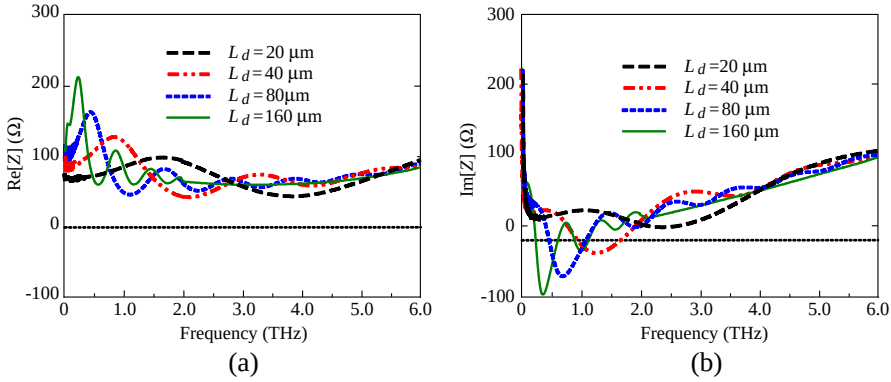

Figure 7. Input impedance of the antenna with different center dipole lengths ($L_b = 8000\,\mu$m): (a) real part and (b) imaginary part.

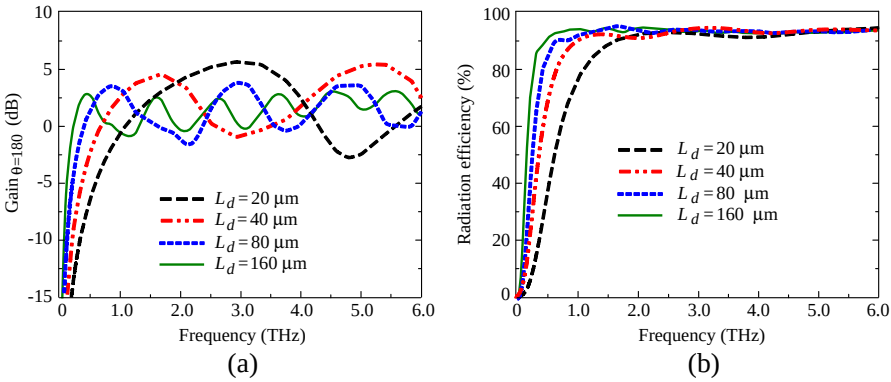

Figure 8. (a) Gain and (b) efficiency of the antennas with different center dipole lengths ($L_b = 8000\,\mu$m).

better impedance bandwidth. The mechanism is expected from the traveling wave behavior along the center dipole length, similar to the behavior of the bias line. It is interesting to note that the antenna gain response shows some unique properties, as illustrated in Figure 8(a). As the center dipole length increased, the gain spectrum exhibited more peaks in the frequency range of interest. The frequencies of the first peak gradually decreased with an increase in the center dipole length. Consequently, the amplitudes of the variations of the antenna gain were gradually reduced for the longer center dipoles. For instance, the amplitudes of variations of the antenna gain were approximately 8.3 dBi for $L_d = 20\,\mu$m, 7.2 dBi for $L_d = 40\,\mu$m, 5.2 dBi for $L_d = 80$,

and 3.4 dBi for $L_d = 160\,\mu m$. The average values of the antenna gain were almost similar for all the cases studied. This indicates that a flat gain with a small variation to support a wideband characteristic could be obtained by using a very long center dipole. In addition, the lower cut-off frequency of the antenna efficiency decreased with an increase in the center dipole length (see Figure 8(b)). For instance, the frequency for saturation of the antenna efficiency was approximately of 2.8 THz for $L_d = 20\,\mu m$, 1.6 THz for $L_d = 40\,\mu m$, 0.8 THz for $L_d = 80\,\mu m$, and 0.4 THz for $L_d = 160\,\mu m$. This allows the antenna to work well even at the very low frequencies.

4. CONCLUSIONS

We investigated the length effects of the DC bias striplines and the center dipole in a typical THz coplanar stripline dipole antenna. The antenna was designed on a semi-infinite substrate and was driven by a constant voltage source. These analysis approaches are needed to characterize the antenna properties itself without mutual effects of the lens substrate and the photoconductive material. The results show that the short bias line acts as an end capacitance and affects the change in the antenna resonance frequency. As the bias line length increases, the antenna takes on a traveling wave structure and produces stable input impedances and minimal changes in the radiation patterns. Moreover, stable gain and efficiency, with frequency-independent behavior, was achieved for sufficiently long bias lines. These investigations explain the mechanisms underlying the preferable use of several-millimeter-length DC bias striplines in the design of typical THz coplanar stripline dipole antennas. In addition, interesting characteristics related to the center dipole length have been found. The long center dipole could also effectively function as a traveling wave structure. Therefore, a very long center dipole is expected to produce a flat gain variation and thus exhibit excellent wideband antenna characteristics. Moreover, this study suggests that a square H-shaped electrode geometry is the most preferred structure for improved gain and efficiency with effective use of the available substrate lens area. This study states that the antenna has to be carefully designed and its frequency response has to be tuned to the frequency range of the photoconductive material response for the optimum overall performance of the device.

ACKNOWLEDGMENT

This work was supported by a National Research Foundation of Korea grant funded by the Korean Government (Grant Code: 2009-0083512).

REFERENCES

1. Jayaraman, S. and C. H. Lee, "Observation of three photon conductivity in CdS with mode locked Nd: Glass laser pulse," *J. Appl. Phys.*, Vol. 44, No. 12, 5480–5482, 1973.
2. Lee, C. H., "Picosecond optoelectronic switching in GaAs," *Appl. Phys. Lett.*, Vol. 30, 84–86, 1977.
3. Auston, D. H., "Picosecond optoelectronic switching and gating in silicon," *Appl. Phys. Lett.*, Vol. 26, 101–103, 1975.
4. Auston, D. H., K. P. Cheung, and P. R. Smith, "Picosecond photoconducting Hertzian dipoles," *Appl. Phys. Lett.*, Vol. 45, No. 3, 284–286, 1984.
5. Grischkowsky, D., I. N. Duling, III, J. C. Chen, and C.-C. Chi, "Electromagnetic shock waves from transmission lines," *Phys. Rev. Lett.*, Vol. 59, No. 15, 1663–1666, 1987.
6. Yang, T., S. Song, H. Dong, and R. Ba, "Waveguide structures for generation of terahertz radiation by electro-optical process in GaAs and $ZnGeP_2$ using 1.55 μm fiber laser pulses," *Progress In Electromagnetics Research Letters*, Vol. 2, 95–102, 2008.
7. Andres-Garcia, B., L. E. Garcia-Munoz, D. Segovia-Vargas, I. Camara-Mayorga, and R. Gusten, "Ultrawideband antenna excited by a photomixer for terahertz band," *Progress In Electromagnetics Research*, Vol. 114, 1–15, 2011.
8. Zyaei, M., A. Rostami, H. Haji Khanmohamadi, and H. Rasooli Saghai, "Room temperature terahertz photodetection in atomic and quantum well realized structures," *Progress In Electromagnetics Research B*, Vol. 28, 163–182, 2011.
9. O'Shea, P. G. and H. P. Freund, "Free-electron lasers: Status and applications," *Science*, Vol. 292, 1853–1858, 2001.
10. Mineo, M. and C. Paoloni, "Comparison of THz backward wave oscillators based on corrugated waveguides," *Progress In Electromagnetics Research Letters*, Vol. 30, 163–171, 2012.
11. Wei, S., J. Weili, and J. Wanli, "Investigation of ultra-wideband electromagnetic radiation based on Si-GaAs photoconductive switches," *Microw. Opt. Tech. Lett.*, Vol. 54, No. 4, 900–904, 2012.
12. Maraghechi, P. and A. Y. Elezzabi, "Experimental confirmation of design techniques for effective bow-tie antenna lengths at THz frequencies," *J. Infrared Milli. Terahz. Waves*, Vol. 32, 897–901, 2011.
13. Brown, E. R., A. W. M. Lee, B. S. Navi, and J. E. Bjarnason, "Characterization of a planar self-complementary square-spiral

antenna in the THz region," *Microw. Opt. Tech. Lett.*, Vol. 48, No. 3, 524–529, 2006.

14. Tani, M., S. Matsuura, K. Sakai, and S. Nakashima, "Emission characteristics of photoconductive antennas based on low-temperature-grown GaAs and semi-insulating GaAs," *Appl. Opt.*, Vol. 36, No. 30, 7853–7859, 1997.
15. Miyamaru, F., Y. Saito, K. Yamamoto, T. Furuya, S. Nishizawa, and M. Tani, "Dependence of emission of terahertz radiation on geometrical parameters of dipole photoconductive antennas," *Appl. Phys. Lett.*, Vol. 96, No. 21, 211104, 2010.
16. Diao, J., F. Yang, L. Du, J. Ouyang, and P. Yang, "Enhancing terahertz radiation from dipole photoconductive antenna by blending tips," *Progress In Electromagnetics Research Letters*, Vol. 25, 127–134, 2011.
17. Maraghechi, P. and A. Y. Elezzabi, "Enhanced THz radiation emission from plasmonic complementary Sierpinski fractal emitters," *Opt. Express*, Vol. 18, No. 26, 27336–27345, 2010.
18. Diao, J. M., F. Yang, Z. P. Nie, J. Ouyang, and P. Yang, "Separated fractal antennas for improved emission performance of terahertz radiations," *Journal of Electromagnetic Waves and Applications*, Vol. 26, Nos. 8–9, 1158–1167, 2012.
19. Dragomana, D. and M. Dragomanb, "Terahertz fields and applications," *Progress in Quan. Electron.*, Vol. 26, No. 1, 1–66, 2004.
20. Van Exter, M. and D. Grischkowsky, "Characterization of an optoelectronic terahertz beam system," *IEEE Trans. Microwave Theory Tech.*, Vol. 38, No. 11, 1684–1691, 1990.
21. Harde, H. and D. Grischkowsky, "Coherent transients excited by subpicosecond pulses of terahertz radiation," *J. Opt. Soc. Am. B*, Vol. 8, 1642–1651, 1991.
22. BATOP GmbH, http:/www.batop.de/.
23. Shafai, L. and S. Noghanian, *Modern Antenna Handbook*, C. A. Balanis (ed.), Chapter 9, Wiley, 2008.
24. Chen, H.-T., J.-X. Luo, and D.-K. Zhang, "An analytic formula of the current distribution for the VLF horizontal wire antenna above lossy half-space," *Progress In Electromagnetics Research Letters*, Vol. 1, 149–158, 2008.
25. Kominami, M., D. M. Pozar, and D. H. Schaubert, "Dipole and slot elements and arrays on semi-infinite substrate," *IEEE Trans. Antennas Propagat.*, Vol. 33, No. 6, 600–607, 1985.
26. Nguyen, T. K., T. A. Ho, H. Han, and I. Park, "Numerical study

of self-complementary antenna characteristics on substrate lenses at terahertz frequency," *J. Infrared Milli. Terahz. Waves*, Vol. 33, No. 11, 1123–1137, 2012.

27. Nguyen, T. K. and I. Park, "Resonant antennas on semi-infinite and lens substrates at terahertz frequency," *Convergence of Terahertz Sciences in Biomedical Systems*, 181–193, G.-S. Park, Ed., Springer, 2012.
28. Van Rudd, J. and D. M. Mittleman, "Influence of substrate-lens design in terahertz time-domain spectroscopy," *J. Opt. Soc. Am. B*, Vol. 19, No. 2, 319–329, 2002.
29. Rutledge, D. B. and M. S. Muha, "Imaging antenna arrays," *IEEE Trans. Antennas Propagat.*, Vol. 30, No. 4, 535–542, 1982.
30. Tonn, D., "Radiation patterns of standing wave and traveling wave microstrip dipoles," Master's Thesis, University of Connecticut, 1994.
31. Coleman, C., *An Introduction to Radio Frequency Engineering*, 258–259, Cambridge University Press, Cambridge, New York, 2004.